Biophysics and Physicobiology

Regular Article

Genetic analysis of revertants isolated from the rod-fragile *fliF* mutant of *Salmonella*

Hitomi Komatsu[1]*, Fumio Hayashi[2]*, Masahiro Sasa[3], Koji Shikata[3], Shigeru Yamaguchi[4], Keiichi Namba[1,5] and Kenji Oosawa[1,2,3]

[1]*Protonic NanoMachine Project, ERATO, JST, Seika, Kyoto 619-0237, Japan*
[2]*Division of Molecular Science, Faculty of Science and Technology, Gunma University, Kiryu, Gunma 376-8515, Japan*
[3]*Department of Biosciences, Teikyo University, Utsunomiya, Tochigi 320-8551, Japan*
[4]*Izumi Campus, Meiji University, Suginamiku, Tokyo 168-8555, Japan*
[5]*Graduate School of Frontier Biosciences, Osaka University, Suita, Osaka 565-0871, Japan*

FliF is the protein comprising the MS-ring of the bacterial flagellar basal body, which is the base for the assembly of flagellar axial structures. From a *fliF* mutant that easily releases the rod-hook-filament in viscous environments, more than 400 revertants that recovered their swarming ability in viscous conditions, were isolated. The second-site mutations were determined for approximately 70% of them. There were three regions where the mutations were localized: two in Region I, 112 in Region II, and 71 in Region III including the true reversion. In Region I, second-site mutations were found in FlgC and FlgF of the proximal rod, suggesting that they affect the interaction between the MS-ring and the rod. In Region II, there were 69 and 42 mutations in MotA and MotB, respectively, suggesting that the second-site mutations in MotA and MotB may decrease the rotational speed of the flagellar motor to reduce the probability of releasing the rod under this condition. One exception is a mutation in FlhC that caused a down regulation of the flagellar proteins production but it may directly affect transcription or translation of *motA* and *motB*. In Region III, there were 44, 24, and 3 mutations in FliG, FliM, and FliF, respectively. There were no second-site mutations identified in FliN although it is involved in torque generation as a component of the C-ring. Many of the mutations were involved in the motor rotation, and it is suggested that such reduced speeds result in stabilizing the filament attachment to the motor.

* These authors equally contributed.
Corresponding author: Kenji Oosawa, Faculty of Science and Technology, Gunma University, 1-5-1 Tenjin-cho, Kiryu, Gunma 376-8515, Japan.
e-mail: kenji@gunma-u.ac.jp

Key words: bacterial flagellum, revertant, MS-ring, rod, motor

Salmonella flagellum is a biological nanomachine that makes it possible for a bacterial cell to swim freely. The flagellum is a huge protein assembly consisting of approximately 30 kinds of proteins. It consists of three major parts with distinct functions: the basal body, acting as a rotary motor as well as a flagellar protein export apparatus; the long helical filament, working as a helical propeller; and the hook, connecting the basal body and the filament to function as a universal joint. A schematic diagram of the flagellar basal body is shown in Figure 1. It has been believed that the assembling process of the flagellum starts from the formation of a ring structure embedded in the cytoplasmic membrane called the MS-ring [1]. Recently, an alternative model was proposed, that the initiation step is oligomerization of FlhA as a scaffold, followed by the recruitment of the MS-ring [2]. In either model, the MS-ring formation in the inner membrane is involved in one of the earliest steps in the flagellum construction. The MS-ring consists of approximately 26 subunits of a 61 kDa protein FliF with a rotational symmetry [3–6]. All other flagellar proteins are assembled sequentially around the MS-ring. The assembly surrounding the MS-ring in the inner membrane is called the stator or MotAB complex composed of MotA (four subunits) and MotB (two subunits) [7], and the cytoplasmic assembly docking into the MS-ring is called C-ring composed of FliG (~26 subunits), FliM (~34 subunits) and FliN (110~140 sub-
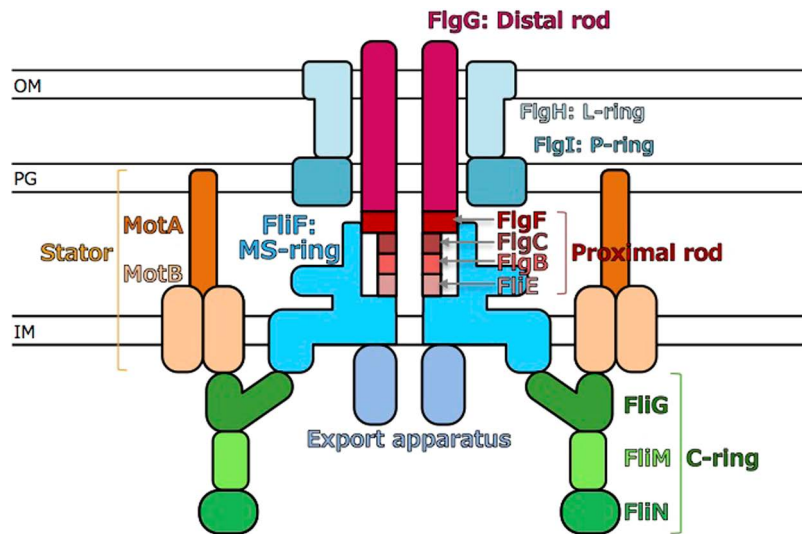
Figure 1   Schematic diagram of the flagellar basal body. Substructures and proteins constructing these substructures are indicated in different colors and labeled with corresponding colors.

units) [6, 8–10]. The C-ring, working as a rotor of the flagellar motor, binds to the MS-ring *via* the first 46 amino acids of FliG [11], whereas the MotAB complex, working as a stator, does not bind to the MS-ring, but interacts weakly with the C-ring *via* the C-terminal domain of FliG [12–14]. The outward assembling processes involve the rod, the hook, and the filament. The rod is separated into two regions, the proximal rod consisting of FlgB (6 subunits), FlgC (6 subunits), and FlgF (6 subunits) and the distal rod consisting of FlgG (26 subunits) [15,16]. FlgB connects to the MS-ring *via* the ring-rod adapter FliE (9 subunits) [16]. It is unknown how FlgC and FlgF are constructed in the proximal rod. The distal rod consisting of FlgG connects the proximal rod to the hook [17]. At the distal end of the hook, the flagellar filament is assembled onto the junction with proteins HAP1 and HAP3 [19].

Proton influx through the MotAB complex induces the C-ring rotation. The rotation direction is regulated by stimuli, the attracting one induces counter-clockwise (CCW) rotation (as it is viewed from outside the cell) causing smooth swimming and the repelling one induces clockwise rotation introducing tumbling. When repellent signals from chemicals [20–22] and temperature [23,24] are sensed by the receptors embedded in the inner membrane [25], the signaling protein CheY is phosphorylated (CheY-P) [26,27]. Upon binding of the CheY-P to FliM, the CCW rotation of the C-ring rapidly inverts about a tenth of a second [28]. Such C-ring rotation generated inside the cell drives the filament rotation in the cell exterior by the transmembrane protein complex MS-ring. Thus, MS-ring is functioning both as a nucleus for flagellation and a power transmission device between the C-ring rotation and the flagellar filament rotation.

Okino *et al.* found a unique *fliF* mutant of *Salmonella*, SJW3060, which showed the following properties; 1) swimming speed and tumbling frequency were the same as those of the wild-type cells in liquid medium as a non-viscous condition; 2) swarm rate was very low in a semisolid agar plate containing gelatin as a viscous condition; 3) filament-hook-rod (FHR) complexes (composed of the filament, the filament-hook junctions, the hook, and the distal rod) were detached from the cells in a viscous medium [17]. From these results, it was thought that SJW3060 had weak interactions between the MS-ring and the distal rod, which were destroyed by a little higher load against motor rotation [17].

From the results of analyses of flagellar assembling processes [29], it is difficult to figure out how the MS-ring interacts directly to the distal rod, and the role of the proximal rod is still unknown. To examine the interaction between the MS-ring and the distal rod and to find the role of the proximal rod, we isolated revertants from the rod fragile mutant SJW3060. By the revertant isolation, we expected to find flagellar proteins interacting directly with the MS-ring protein FliF. As a result, we isolated many revertants, a few of them were mapped in the genes for the proximal rod proteins and the rests were in other flagellar genes relating with motor functions, such as the *mot* genes and the genes for the C-ring proteins. Here we report that the defects of the rod fragile mutant SJW3060 are recovered by not only mutations in the proximal rod proteins but also mutations related with motor functions.

Materials and Methods

Strains, plasmids, and phages

Salmonella enterica serovar Typhimurium strains used in this study are derivatives from LT2. The rod-fragile mutant SJW3060 is a derivative of SJW1103 [17] and other *Salmonella* strains used for mapping of second-site mutation were

#162 and SJW98 for the flagellar genes Region I and II, respectively (Yamaguchi, unpublished data). Plasmid pBR322 and pHSG395 were used for cloning of DNA fragments amplified with PCR [30]. Bacteriophage P22 was used for transductions of Tn10 inserted flagellar genes into SJW3060 and for mapping second-site mutation by transduction [31,32].

Media

Cells were grown in Luria-Bertani broth (LB broth) containing 1% Tryptone (Difco), 0.5% yeast extract (Difco), and 1% NaCl. LB plate and LB soft agar plate contain 1.5% and 0.3% Agar (Difco) in LB broth, respectively. LGA plate contains 8% gelatin in LB soft agar plate.

Isolation of revertants

A large number of single colonies of SJW3060 on LB plates were stabbed onto LGA plates and incubated at 37°C overnight. Occasionally, swarms appeared from the edge of the stabs. The cells were picked from the fringe of each swarm which was only one swarm for each stabbed point and then were streaked on LB plates. A single colony from each swarm was tested.

Preparation of the recipients for mapping of second mutations of the revertants

Salmonella flagellar genes are located on four regions: Region I containing *flgA*, *B*, *C*, *D*, *E*, *F*, *G*, *H*, *I*, *J*, *K*, *L*, *M*, and *N*, Region II containing *flh A*, *B*, *C*, *D*, and *E*, *cheA*, *B*, *R*, *W*, *Y*, and *Z*, *motA* and *B*, Region III containing *fliA*, *B*, *C*, *D*, *E*, *F*, *G*, *H*, *I*, *J*, *K*, *L*, *M*, *N*, *O*, *P*, *Q*, *R*, *S*, *T*, and *Z*, and Region IV containing *fljA*, *B*, *and hin* [33–35]. We assumed that the second-site mutations occurred within Regions I–III. To determine which region contains the second mutations, we applied bacteriophage P22-mediated transduction method [31,32]. For the assay, we first prepared two recipients; one was termed as RI recipient, which was SJW3060 lacking a part of Region I, and another was termed as RII recipient, which was SJW3060 lacking a part of Region II. Since the original mutation in SJW3060 is located in Region III, introduction of deletion in Region III by transduction into SJW3060 may cause co-transduction of wild-type *fliF* with deletion. Therefore, we excluded Region III from the P22-mediated transduction method.

P22 phage lysate from #162 strain (*flgG*::Tn10) was mixed with SJW3060 culture. The mixture was spread on LB-Tet plates (LB-plate containing tetracycline (25 mg/L)) to select tetracycline-resistant transductants. The colonies appeared on the LB-Tet plate were tested as non-motile on the LB soft agar plate. The tetracycline-resistant non-motile transductants were cultured in LB broth overnight, and then the culture was spread on a Bochener selection plate [36] to select cells spontaneously lacking Tn10 from the transductants. Colonies that appeared on the plate were inoculated onto both an LB plate and an LB-Tet plate for testing tetracycline-resistance. After overnight incubation, the colonies appeared on the LB plate but not on the LB-Tet plate were collected as candidates of RI recipient. RI recipient was confirmed in that it could not form a swarm at all because of deletion in Region I derived from Tn10 excision. Similarly, RII recipient was prepared using P22 phage lysate from SJW98 (*flhC*::Tn10).

Mapping

The revertants were crossed with the RI or RII recipient. If the second-site mutation of the revertant was located in Region I, only the RI recipient receiving the DNA fragment from the revertant by P22 phage transduction formed swarms. If the second-site mutation was located in Region II, the RII recipient formed swarms. When crossing with both types of recipients did not generate any swarms, it was classified that the second mutation site might be located in Region III.

The P22 phage lysate from the revertant was streaked as a line on LGA plate, and then overnight culture of the RI or RII recipient was cross-streaked on the trail of the P22 phage lysate. After overnight incubation at 37°C, we checked whether spontaneous swarms extending as flares from the main growth lines appeared or not.

Determination of the mutation site of SJW3060 and the second-site mutations of the revertants

It has been determined that SJW3060 carried mutation only in *fliF* gene (Yamaguchi, unpublished data). The original mutation of SJW3060 was determined by DNA sequencing analysis. The DNA fragment containing *fliF* was amplified by polymerase chain reaction (PCR) using two primers surrounding the *fliF* gene and the genome DNA prepared from SJW3060 as a template. DNA sequencing samples were prepared using the purified PCR product as a template, the appropriate sequence primers, and ABIPRISM big dye terminator (Applied Biosystems).

The second mutation sites of the revertants were determined by exhaustive survey of the DNA sequence of the regions indicated by the mapping results. The entire length of Region I, II, or III was amplified by PCR using *Hind*III site-conjugated primers and the genome DNA prepared from each revertant, and then the PCR products were cloned into pBR322. The inserted DNAs were digested by combinations of appropriate restriction enzymes, and the resultant fragments were cloned into pHSG395. DNA sequencing samples were prepared using the plasmids as a template, M13 and the appropriate sequence primers, and ABIPRISM big dye terminator. DNA sequencing was performed using an ABI377 sequencer (Applied Biosystems).

Prediction of the secondary structure

The secondary structures of FliF, FlgC, and FlgF were predicted by the PSIPRED secondary structure prediction algorithm [37].

Results

Identification of the original mutation of SJW3060

DNA fragment containing the *fliF* gene from SJW3060 was sequenced. There was only a single nucleotide difference from that of the wild-type *fliF* gene, C at 953 from the start codon replaced with A. The resulting amino acid substitution of FliF in SJW3060 was N318T. This result is consistent with that determined by H. Sockett and R. M. Macnab (personal communication). As described previously, the region containing N318 was not predicted as any discrete secondary structure but may localize to the interface with the rod structure [1,5,38].

Mapping second-site mutations using P22 transduction

We isolated 468 cells that formed swarm rings from the stabbed point of SJW3060 in LGA plates. All the isolates were tested for P22 phage transduction with the RI and RII recipients, which is SJW3060 carrying a deletion in Regions I and II in the flagellar genes, respectively. As a result, five of the RI recipients and 208 of the RII recipients recovered a swarming ability on LGA after transduction. The remaining 255 did not recover in both cases. In Figure 2, swarms of some representatives in each group on LGA are shown with those of SJW1103 and SJW3060. The revertants in the first and second groups were subjected to DNA sequencing in Regions I and II, respectively. Since the remaining revertants most likely had the second mutations in Region III, they were subjected to DNA sequencing only in that region.

Second-site mutations in Region I

All of the second-site mutations were determined by DNA sequencing. Three of them were in the *flgC* gene, which encodes one of the proximal rod proteins and two were in the *flgF* gene encoding also another proximal rod protein. Three mutation sites in *flgC* were identical, and the resulting amino acid substitution was FlgC$_{V48F}$. Two sites in *flgF* were identical, and the substitution was FlgF$_{H3R}$.

Second-site mutations in Region II

DNA sequencing of 208 revertants that mapped to Region II revealed that 102 and 81 of the second-site mutations were in the *motA* and *motB* genes, respectively. The amino acid substitutions derived from those mutations are summarized in Table 1. A few of them were isolated repeatedly, although most were isolated only once. In addition, four revertants in Region II carried their second-site mutations in the *flhC* gene which is one of the master operon genes regulating transcription level of flagellar genes. The mutated gene encodes the FlhC$_{I188S}$ protein. We did not identify mutations in 21 revertants mapped to Region II.

Second-site mutations in Region III

The revertants that recovered swarming ability of neither RI nor RII recipients on the LGA plates upon transduction were judged to carry their second mutations neither in Region I nor II. Since restoration of the function for swarm ability in the viscous condition is most likely related with flagellar function, possible candidates for the site of second mutations are genes in Region III. So, we decided that DNA sequencing should be done throughout Region III. About half of them were determined to carry their second-site mutations in the *fliG* and *fliM* genes, which are two of the three genes encoding the components of the C-ring. The second-site mutations of 89 revertants were in *fliG* and 44 were in *fliM* (Table 1). A few of them were isolated more than once, although most were isolated once. There were only four revertants whose second-site mutations were identified in the *fliF* gene. Two were true revertants and one was a pseudo-revertant encoding FliF$_{G307C}$. Another pseudorevertant had FliF$_{N318A}$, which is the same amino acid site as the original mutation of SJW3060 but mutated to Ala instead of Asn. For the remaining 118 revertants, there was no mutation site identified by DNA sequencing.

Discussion

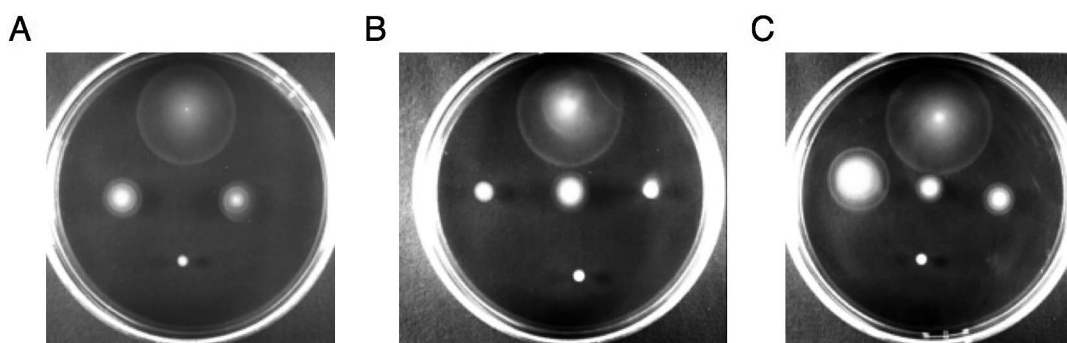SJW3060 swims as fast as wild type in the liquid medium;

Figure 2 Swarms of representative pseudorevertants on semisolid agar plates. (A) Pseudorevertants mapped in Region I. (B) Pseudorevertants mapped in Region II. (C) Pseudorevertants mapped in neither Region I nor Region II. Each panel shows swarms on LGA: top, the wild-type SJW1103; middle, pseudorevertants; bottom, the original mutant SJW3060.

Table 1   The second mutations of SJW3060-revertants on MotA, MotB, FliG, and FliM

MotA		MotA		MotB		FliG		FliM	
I3L	1	A179V	1	H24R	1	A131T	2	R60L	1
Y7C	1	G183E	4	G25V	1	E151K	1	R66Q	3
G17A	2	A187G	1	S26F	2	N204D	1	F70L	1
G17C	1	A187S	1	S26Y	1	D231G	2	L72P	2
G22A	3	D192A	1	K28N	1	D243G	2	L72Q	1
G23R	1	D192E	1	K28R	13	D243N	2	A93E	1
P31A	2	D192Y	1	A30P	1	D243V	1	N101K	1
P31S	3	E197V	1	Y31C	5	D244A	1	L102Q	2
E33K	1	L198F	1	Y31N	3	S246I	1	N103S	1
A40E	1	L201V	1	A37V	2	S246N	1	L104Q	10
A40P	1	M206I	1	A40T	1	Q248P	1	L104R	4
A44E	1	V207A	2	V44A	1	I261N	4	L115Q	1
A44V	2	T209A	4	I127N	1	I261S	1	F124L	4
F45L	2	G212A	1	N158S	1	A262T	1	E145A	1
G48S	1	I213M	1	R159S	1	A262V	2	E145K	1
N50K	1	L215P	2	G165S	1	K264N	1	S182P	1
P62L	1	F219C	1	E170K	3	E267D	1	E183A	1
T71I	1	F219L	1	A181E	1	R281S	1	M184R	1
M76V	1	L223S	1	N185S	1	A283T	1	Q185P	1
L78W	1	V226F	1	A194T	1	P295Q	1	K187T	1
Y83C	3	R228C	1	P201T	1	P295S	2	F188S	1
Y83H	1	K236N	1	A203T	2	V296A	12	T189N	1
I126F	1	C240S	1	G205C	3	V296D	6	T192P	2
R131H	1	L246Q	1	G205S	1	R297C	1	P234S	1
R131L	1	P254L	1	K207N	1	R297H	1		
A145E	1	P254S	3	G208D	1	R297P	1		
T153I	1	I256T	1	S210G	1	R297S	4		
E155K	3	T264K	1	E213G	4	S299F	1		
D170G	4	L265F	4	R224C	2	S299P	2		
D170N	1	S268C	1	R224H	1	S299Y	1		
P173A	1	E269G	1	R224S	1	V301E	1		
P173S	2	E275A	1	G234V	1	V301L	1		
G176S	2	H279L	1	K235E	2	V312M	1		
A179E	1	Q288*	2	G241C	2	L315Q	4		
A179S	3			G241S	4	G319C	1		
				A243G	2	G319S	1		
				A244T	2	D328A	1		
				D250Y	2	D328N	1		
				R251G	1	Y330C	5		
				D255G	1	Y330D	3		
				D255Y	2	Y330H	2		
				A256V	2	Y330N	4		
						V331A	4		
						V331D	1		

The second mutations and their number are shown in left and right columns, respectively.
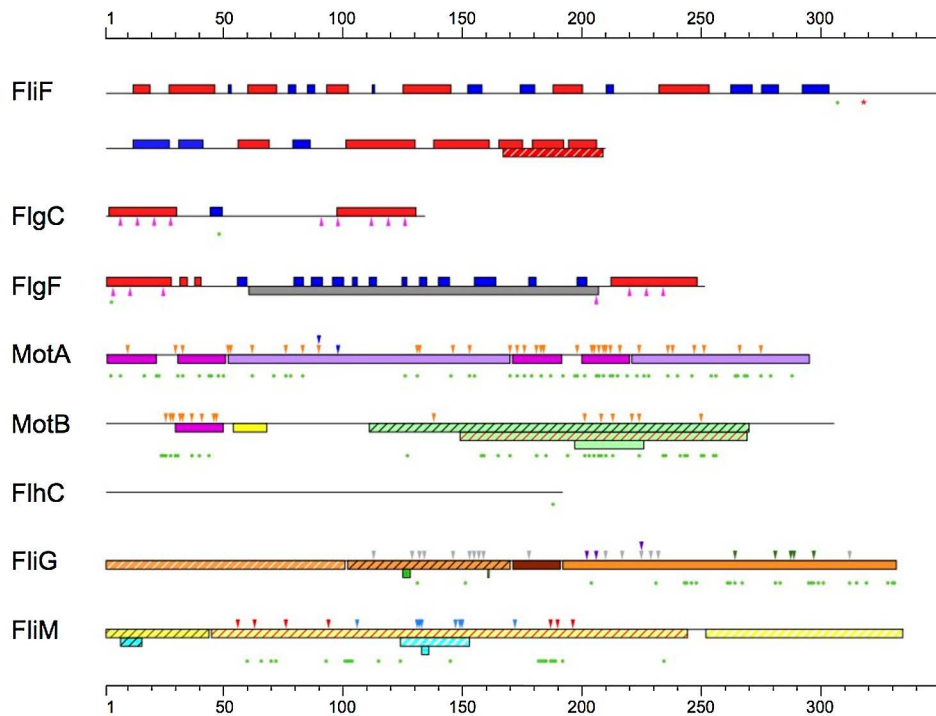
Figure 3   The schematic diagrams of FliF, FlgC, FlgF, MotA, MotB, FlhC, FliG, and FliM of *Salmonella*. The rulers at the top and bottom show amino acid residue number. Since FliF amino acid sequence is long, its schematic diagrams are displayed as two lines. The mutation site of SJW3060 and the all second mutation sites are shown by a magenta asterisk and green closed circles, respectively. The red and blue squares represent predicted α-helices and β-strands, respectively. The gray square represents a compactly folded region [39]. The magenta arrow-heads indicate the positions of heptad repeat of hydrophobic residues [19]. The magenta, violet, and yellow squares represent the transmembrane, the large cytoplasmic, and the plug regions, respectively [42–46]. The pale green squares with black diagonals, red diagonals, and none represent PEM region, OmpA-like domain, and a peptidoglycan binding motif, respectively [57,58]. The orange and the blue arrow-heads indicate the second mutation sites of SJW2811-revertants [40] and the charged residues involved in FliG interaction [14,55], respectively. The orange squares with white diagonals, black diagonals, and no pattern represent the N-terminal, the middle, and the C-terminal domain of FliG, respectively [64]. The brown and green squares represent helix E and EHPQR motif, respectively [65,66]. The gray and purple arrow-heads indicate the FliM binding sites revealed by yeast-two-hybrid assay [69] and by pull-down and Cys-cross-linking assay [67], respectively. The green arrow-heads indicate the charged residues involved in the MotA interaction [68]. The light yellow squares with black diagonals, red diagonals, and white diagonals represent the N-terminal, the middle, and the C-terminal domain of FliM, respectively [75]. The sky-blue squares with black diagonals, white diagonals, and no pattern represent the CheY-P binding region [72,74], the interface to FliGc [67], and the GGXG motif [75], respectively. The red and royal-blue arrow-heads indicate the FliM$_M$-FliM$_M$ interaction sites [75,76] and the single mutation sites leading to *Mot*-phenotype mutants [79].

however, its swarm size is smaller than that of wild type in the LGA plate, and it cannot swim in viscous conditions [17]. The notable phenotype of SJW3060 is that the filament-hook-rod (FHR) complexes are released from the cell bodies under viscous conditions, and the FHR complex thus obtained contains only FlgG proteins as part of the rod [17]. Therefore, Okino *et al.* suggested that the mutation in *fliF* of SJW3060 caused a fragile interface between the distal rod and the MS-ring [17]. It is important for further characterization of this defect to analyze it genetically by isolation and characterization of revertants from this mutant.

In this study, we isolated 468 revertants that formed bigger swarms than SJW3060 on the LGA plate and determined a large fraction of their second-site mutations. We identified many of those mutation sites in *motA*, *motB*, *fliG*, and *fliM* genes, and some in *flgC*, *flgF*, *flhC*, and *fliF* genes. We post the sites on the schematic diagram of each protein in which the structural features such as the functional regions and

the notable amino acid residues were summarized (Fig. 3). For comparison with the previous work for the structures and functions of some of the flagellar proteins described above, FliG, FliM, and FliF sequences of *S*. Typhimurium, *Escherichia coli*, and *Thermotoga maritima* were subjected to sequence alignment analysis (Supplementary Fig. S1). Though biochemical assays and structural analyses have been performed using many different bacterial species, such as *E. coli* and *T. maritima*, the amino acid residue numbers are indicated according to those of *Salmonella enterica* in the following Discussion section.

Region I:
FlgC and FlgF

As described previously, the SJW3060 cells released the FHR complex easily, and the simplest explanation of the result is that the interaction between the FliF ring and the rod is weakened by the N318T mutation in the FliF protein.

Since only the FliE protein has been reported as an interaction partner of FliF on its periplasmic surface [16], this does not appear to be a plausible mechanism. However, the *in situ* structures of the flagellar basal body of a spirochete, *Borrelia burgdorferi*, visualized by electron cryomicroscopy in its various assembly stages suggested direct interactions of rod proteins FlgB and FlgC with the FliF ring [18]. We envisage that a conformational change of FliF induced by the N318T mutation might induce conformational changes in any or all of FliE, FlgB and FlgC through the interactions with the mutant FliF protein. Then the accumulation of those conformational changes may propagate to FlgF and FlgG and eventually weaken the interactions between the rod and FliF at the proximal surface of the FlgG rod portion, causing the FHR complex to detach from the cells. So the second-site mutations identified in the proximal rod proteins FlgC and FlgF might indicate direct interactions between those second mutation sites of the rod proteins and threonine at 318 of the MS-ring protein FliF.

The second mutation site in FlgF was His3, which is located at the predicted α-helix responsible for building the rod structure [19,39] (Fig. 3), suggesting the possibility that the replacement of His to Arg at the site strengthens the interaction of FlgF with the MS-ring. The second mutation site in FlgC was Val48, which is located within the only one β-strand predicted (Fig. 3). Although FlgC is disordered in isolated monomeric form [39], the region around the Val48 might cancel the conformational distortion of the mutant FliF protein by β-strand formation in an assembled form. For further investigation whether these two rod proteins interact directly with the MS-ring protein, it is necessary to construct mutants carrying only the second mutations and perform reversion analysis from them.

The released FHR complex contained only FlgG as the rod protein and there was no evidence for the presence of any of the proximal rod proteins [17]. If the connection between the proximal rod and the MS-ring is broken in SJW3060 under viscous conditions, it is unlikely that the proximal rod protein in the FHR is undetectable. It is, however, possible that the proximal rod is unstable on the FHR or that the conformational instability of the proximal rod induces the disruption in the binding interaction of the distal rod with the MS-ring.

Region II:
MotA and MotB

The number of the second mutation sites in the *motA* gene was 69 at 55 amino acid residues, and some of them were isolated repeatedly, with the highest frequency of 4 for D170G, G183E, T209A, and L265F (Table 1). These might be kinds of hotspots with higher mutation rates. Moreover, they were widely distributed (Fig. 3), and such a wide distribution of the second mutation sites was also observed in the revertant assay of a *fliG* mutant, SJW2811, which showed slow motility [40]. According to that, the number of the

second mutation sites was 54 in the *motA* gene. Of the second mutation sites identified in *motA* from the revertants of SJW2811 and SJW3060, 14 mutations are common at Asp170, and there were two mutations identical in both studies (Table 1). Since the revertants of SJW2811 showed a wide variety of swimming speeds lower than that of wild type, but a swarming ability similar to that of wild type, the authors suggested that the reduced motor torque of the revertants might change swimming behavior upon a chemotactic response and that the resultant changes of direction increase the swarm rate [40]. Our results, together with those of Togashi *et al.* [40] and Garza *et al.* [41], suggest that many of the second-site mutations in the revertants of SJW3060 impair the intact torque generation mechanism.

MotA consists of 295 amino acid residues including four transmembrane (TM) regions (termed TM1~TM4 from the N-terminus) and two extensive cytoplasmic regions [42–46] (Fig. 3). TM3 and TM4 form a proton-conducting channel together with the TM region of MotB [47–52], and the influx of protons through the channel generates the torque to rotate the C-ring. The cytoplasmic regions are involved in motility [53]. In particular, Arg90 and Glu98 within the first cytoplasmic region are responsible for the interaction with the C-ring protein FliG in installation of the MotAB complex as the stator into the motor and torque generation [14,54,55]. Since some of the second-site mutations were present in these two TM regions, it is suggested that the recovery of swarming on the LGA plate is derived from modification in torque generation by the revertants (Fig. 3).

The number of the second mutation sites in MotB was 42 at 33 amino acid residues, and some of them occurred repeatedly. The highest rate was 13 of K28R, suggesting that there is a possible hotspot for mutation in the *motB* gene. Those second mutation sites were localized in only two regions: one in the transmembrane region and the other in the region located in the periplasmic space. MotB consists of a small N-terminal cytoplasmic region (residues 1–29), single TM helix (30–50), and a large periplasmic region (52–309). The TM region contains Asp33 required for proton translocation through the channel [7]. The large periplasmic region contains a plug region that suppresses proton leakage through the proton channel before the MotAB complex is installed into the motor [56] as well as the Periplasmic region Essential for Motility (PEM) which is involved in the assembly, anchoring, and activation of the stator [57].

The PEM region contains an OmpA-like domain [57,58] and a peptidoglycan binding motif [53,59]. This motif is involved in MotB dimerization [57] and anchoring MotA$_4$MotB$_2$ stator complex to the peptidoglycan to construct the functional motor. The second-site mutations in MotB were located in the PEM region, in particular, OmpA-like domain and the TM region with a cytosolic region just below the cytoplasmic membrane (Fig. 3). This distribution is similar to the results of Togashi *et al.* [40]. Similar to the second-site mutations found in MotA, six mutations were
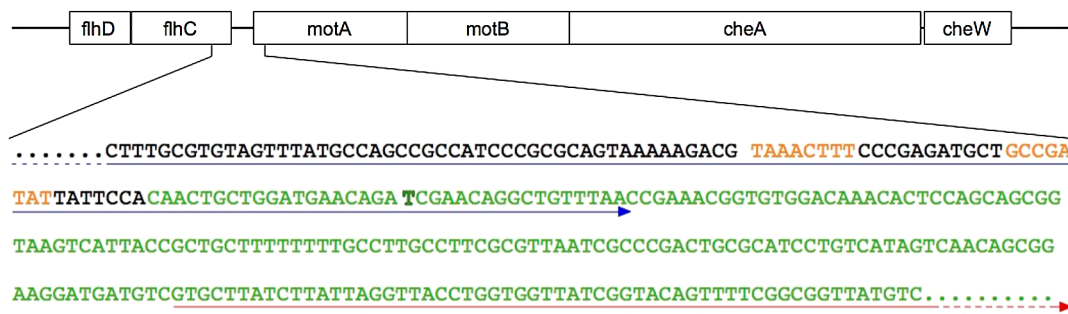
Figure 4   The DNA sequence between *flhC* 3′ and *motA* 5′-regions. The blue and red lines (including each dashed line) indicate open reading frames of *flhC* and *motA*, respectively. The green and orange characters indicate mRNA of *motABcheAW* operon and the *cis* elements of the promoter of the operon, respectively. The bold "T" indicates the second mutation site located in *flhC*.

identical to those of SJW2811, which showed a wide variety of swimming speeds as those in the case of MotA [40]. We isolated second-site mutations in MotA and MotB from the pseudorevertants using P22-mediated transduction and found that most of the seconds-site *motA* and *motB* mutants showed markedly slower swimming speeds in liquid media than the wild type (Supplementary Table S1). These results suggest that some of the second mutation sites identified in MotA and MotB are involved in reducing torque generated by the flagellar motor.

In summary, the second site mutations of MotA and MotB seem to impair torque generation, resulting in the relatively stable attachment of the flagellar filaments under reduced torque, even with the weakened interactions between the MS-ring and the rod.

FlhC

FlhC plays a role as the transcriptional activator for the flagellar class II operons with FlhD [60–63]. Four revertants were identified to have their second-site mutations in the *flhC* gene, but only one mutation, FlhC$_{I188S}$, was determined. FlhC$_{I188S}$ may affect the expression levels of FlgC, FlgF, and FliF. However, it seems to be difficult for just the changes in the expression levels of these proteins to prevent the FHR complexes from detachment. Instead, we suspect that the second-site mutation that occurred in the *flhC* open reading frame might change other factors rather than the substitution of the amino acid sequence of the protein. One idea is that the mutation affects the transcriptional level of mRNA of *motABcheAW* and/or their translation levels, because the *flhC* coding region is overlapped with the promotor of the downstream operon *motABcheAW* and the mutation site is in a part of the non-coding region of the mRNA upstream of these genes (Fig. 4). Considering that there were a large number of MotA and MotB mutations that occurred in SJW3060 revertants (Fig. 3 and Table 1), it is possible that the *flhC* mutation affects the expression levels of MotA and MotB. As a result, the number of MotAB complexes installed into the motor decreases. Since the number of MotAB complexes affects the rotational speed of the flagellar motor

([44] for review), the motor with a reduced number of the MotAB complexes in the revertants cannot rotate so vigorously that the detachment of the FHR complexes are suppressed.

There were approximately 10% of the revertants (21 of 208) whose mutation sites were not identified by DNA sequencing although they were mapped in Region II. We extended our search for the mutations to Region I and Region III, but it was not successful. One possible reason for this problem may be that these revertants may not actually be mutants since the differences in the swarm sizes on LGA were relatively small between these revertants and SJW3060 (data not shown).

Region III:

There were more than 250 revertants that were not mapped in either Region I or Region II in the P22 transduction. We thought that the second-site mutations were in Region III because other genes related with flagellar functions were only in this region except for *flj* genes. So, we investigated them by DNA sequencing over the entire Region III. More than half of the second-site mutations (137 of 255) were identified in Region III. The rest were subjected to the analysis of other flagellar regions, but none of them were determined for the same reason described for those in Region II.

FliG

Only 44 sites for amino acid substitution were found in 89 revertants in FliG and there were 17 sites isolated repeatedly with the highest frequency of 12 for V296A (Table 1). Since the total of 18 revertants were isolated at Val296 (Table 1), it is suggested that the second nucleotide of this codon is a hotspot for mutation. Most of the other second mutation sites found in FliG were located in its C-terminal domain, except for A131T and E151K (Fig. 3). FliG is comprised of three domains and helix E connecting the second and third domains [64] (Fig. 3), each with distinct functions as follows: the N-terminal domain (FliG$_N$) interacts with the MS-ring, the middle domain (FliG$_M$) interacts with FliM [65–67]; the C-terminal domain (FliG$_C$) interacts with the cytoplasmic
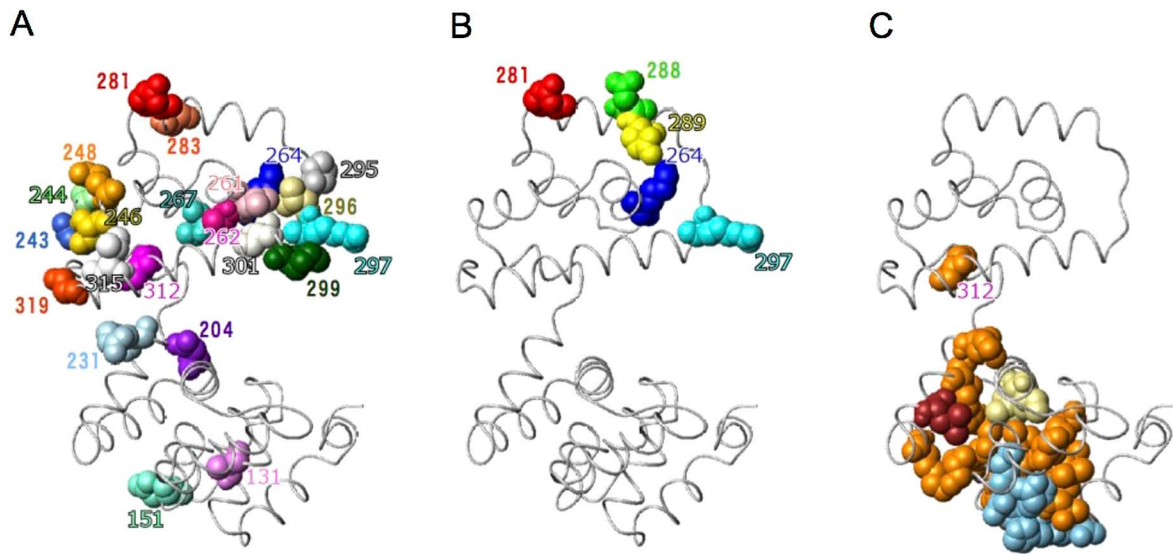
Figure 5   The second mutation sites on FliG$_{MC}$ structure. The backbone structures of *T. maritima* FliG$_{MC}$ (Protein Data Bank accession No. 3AJC) are displayed. (A) The second mutation sites are shown in CPK models with different colors. (B) The five charged residues involved in the MotA interaction [68] are shown by CPK models with different colors (the residues in panels A and B are shown with the same colors). (C) The FliM binding residues revealed by pull-down and Cys-cross-linking assays [67] and the deduced FliM binding residues revealed by yeast-two-hybrid assay [70] are represented by CPK model with khaki and orange colors, respectively. The residue colored with brown is found by all the assays. The residues colored with sky-blue represent the EHPQR motif [65,66]. The numbering is according to the amino acid residue numbers of *Salmonella*.

domain of MotA *via* their conserved charged residues [14,55,68] and FliM *via* a hydrophobic patch [65]; and helix E connects FliG$_M$ to FliG$_C$ and presumably allows the different arrangements of the two domains between CCW and CW rotations [64,65,69].

The second-site mutations in the C-terminal domain were located around the conserved charged residues, Lys264, Arg281, and Arg297, which are responsible for the interactions with MotA [68] (Fig. 5A, B). These results suggest that the second-site mutations in FliG may weaken the interactions with MotA and that the weak interactions reduce the torque generated. Although it has been reported that Asp288 and Asp289 are also important charged residues for the FliG-MotA interaction [68], the second-site mutations did not occur at these two residues. If the second-site mutations occurred at these two residues, the mutations would impair motor rotation and not recover swarming ability in the revertants.

Four of the second mutation sites, Ala131, Glu151, Asn204, and Asp231, were located near the region responsible for the FliG-FliM interaction [65–67,70] (Figs. 3 and 5). How such mutations affect the detachment of the FHR complex will be discussed in the next section.

Four and three second mutation sites were localized to two short segments, one between Asp243 and Gln248 and the other between Val312 and Gly319, respectively (Fig. 3). These two segments are separated relatively far in the primary sequence, but they form one cluster in the opposite side of the conserved charge residues in the tertiary structure (Fig. 5). Although there is little information about this

region, this may have some important roles in the FliG function, or the segment including Val312 may be involved in the FliG-FliM interaction.

FliM

Only 24 sites for amino acid substitution were identified in 44 revertants in FliM and seven sites were isolated repeatedly (Table 1). In particular, the second nucleotide of the codon for Leu at 104 was mutated in 14 independently isolated revertants, suggesting that this nucleotide is a hotspot for mutation. Most of the second mutation sites in FliM were located in the middle of the primary structure, except for P234S (Fig. 3). FliM is comprised of three domains with distinct functions as follows: the N-terminal domain (FliM$_N$) interacts with CheY-P [71–74]; the middle domain (FliM$_M$) interacts with FliG$_M$, FliG$_C$ [67], FliM$_M$ of neighboring FliM subunits [75,76], and CheY-P after interacting with FliM$_N$ [73]; the C-terminal domain (FliM$_C$) interacts with FliN [74] (Fig. 3). In the middle domain, the second-site mutations are located around residues Ile56, Arg63, Ser76, Arg94, Phe188, and Asn190, which are all involved in the FliM$_M$-FliM$_M$ interactions [75] (Figs. 3 and 6), suggesting that these mutations interrupt the assembly of the C-ring. Since the main structural components of the C-ring, i.e., FliM and FliN, coordinate the organization of FliG subunits [67,76], it is reasonable to conclude that certain mutations in FliM affect their interactions with FliG. Furthermore, since FliM subunits in the C-ring are dynamically exchanged in a bacterial cell [77,78], it seems possible that the FliM$_M$-FliM$_M$ interaction sites are very important for stabilizing the C-ring. Alter-
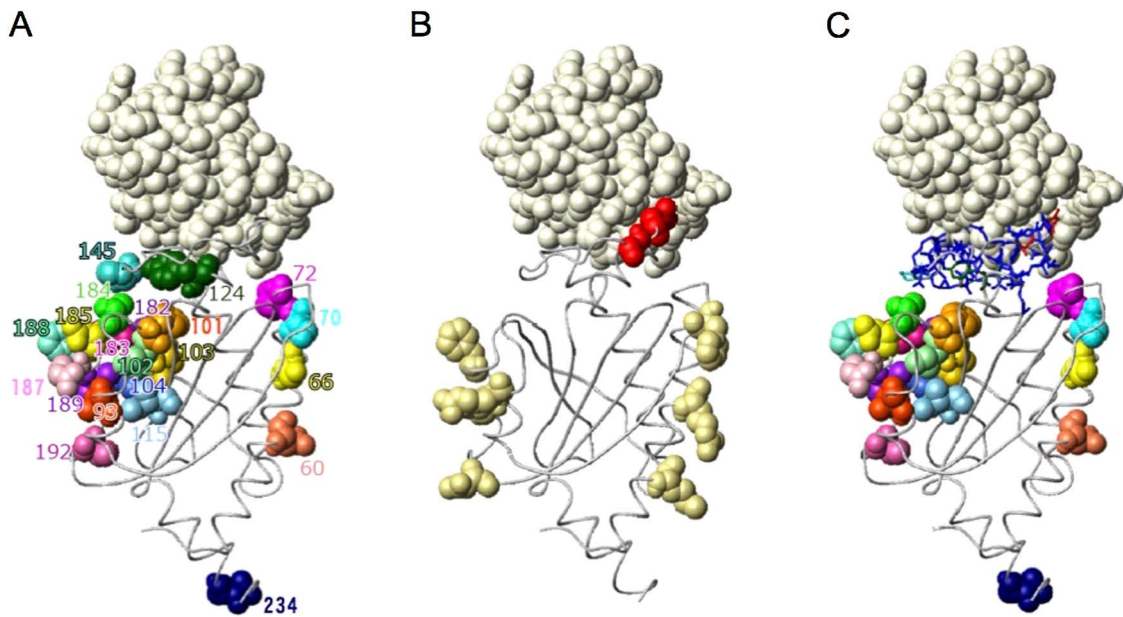
Figure 6   The second mutation sites on FliM$_M$ structure. The structure of *T. maritima* FliG$_M$-FliM$_M$ complex (Protein Data Bank accession No. 3SOH) is shown and FliG$_M$ of the complex is displayed by CPK model with pale yellow. For the FliM$_M$, its backbone structure is displayed. (A) The second mutation sites generated in FliM$_M$ are shown by CPK models with different colors. (B) The six residues colored with khaki is involved in FliM$_M$-FliM$_M$ interaction [75,76], and the residues colored with red represent GGXG motif [75]. (C) The residues between 124th and 153th of FliM$_M$ are represented by stick model. The numbering is according to the amino acid residue numbers of *Salmonella*.

natively, since the six residues mentioned above and Asn196 exchange their interaction partner upon switching of motor rotation between CCW and CW [76], the mutations near the six residues may interfere with the CCW/CW switching of motor.

From the results of the second-site mutations at Phe124 and Glu145, which form the FliM$_M$-FliG$_C$ interface with other residues between residues 124 and 153, including the GGXG motif [75] (Fig. 6C), it is suggested that mutations at these two residues affect the FliM-FliG interactions. The altered FliM-FliG interaction disrupts the organization of FliG [67], and so the defective C-ring cannot rotate as in the wild-type motor. Moreover, in the mutational assay of FliM, some mutations in the interface region result in reductions in their motilities [79]. As described in the section for FliG, some of the second-site mutations in FliG were found in the residues involved in the FliG-FliM interaction. In those cases, it is also thought that FliG subunits are not organized well as in the wild-type C-ring.

FliF

The original mutation of SJW3060 was FliF$_{N318T}$ and one revertant had Ala at the same site. Although amino acid residues, such as Ala and Thr are classified into the same group in many categories, they showed a significant difference in the FliF function. Another second-site mutation found in this protein was FliF$_{G307C}$. In this case, the mutation is located in the predicted long disordered region containing Asn318 (Fig. 3). Although the mechanisms are not clear, this muta-

tion could restore the MS-ring structure distorted by the FliF$_{N318T}$ mutation or through stabilizing the interaction between the MS-ring and the rod within the flagellar motor of the revertant under viscous conditions.

While many of the second-site mutations of the revertants isolated from SJW3060 were found in FliG and FliM, there were none in the FliN protein, which is present at the bottom of the C-ring. FliN interacts with FliM in the C-ring, and its function is mainly to facilitate flagellar protein export [80,81]. Null mutants of the *fliN* gene showed non-motile phenotype, and there has been no report of any *fliN* mutant showing partially defective motility. These findings suggest that mutations in *fliN* may not be able to cause a partial defect in motility, such as a reduced rotational speed of the flagellar motor, to suppress the damage in the basal body structure of SJW3060.

One characteristic phenotype of SJW3060 was the detachment of the FHR complexes from the MS-ring. As a likely scenario, we expected that a large number of revertants had second-site mutations in FliF, FliE, FlgB, FlgC, FlgF, or FlgG that strengthen the interactions between the MS-ring and the rod. However, only four second-site mutations, FlgC$_{V48F}$, FlgF$_{H3R}$, FliF$_{G307C}$, and FliF$_{N318A}$, were identified among these six proteins. To understand the interactions among the rod, the MS-ring, and the rod-ring adapter, it may be useful to conduct mutational analyses of them and suppressor analyses on the FlgC$_{V48F}$, FlgF$_{H3R}$, FliF$_{G307C}$, and FliF$_{N318A}$ mutants as the parental strains. The measurement of the force required to break connections between the prox-

imal and distal rods in wild type, SJW3060 and the four revertants would also be very important to understand the cause of the reversion.

Unexpectedly, many of the second-site mutations were located in MotA, MotB, FliG, and FliM. Considering the available information, these second-site mutations appear to affect the intrinsic rotation ability of the flagellar motor, such as rotational speed and switching of the rotational direction. Measuring the rotational speed of the flagellar motor of each mutant with only the second mutation without the SJW3060 mutation will reveal the sites involved in the intrinsic motor rotation mechanism.

Conclusion

From a *fliF* mutant that easily releases the rod-hook-filament in viscous environments, more than 400 revertants that recovered their swarming ability in viscous conditions were isolated and the second-site mutations were analyzed. Some of the mutations mapped in Region I were involved in the interaction between the MS-ring and the proximal rod, and the rest were involved in the motor rotation.

Acknowledgments

Conflict of Interest

H. K., F. H., M. S., K. S., S. Y., K. N. and K. O. declare that they have no conflict of interest.

Author Contributions

H. K. analyzed DNA sequences of revertants. F. H. performed analyses of protein homology and structural prediction. M. S. and K. S. isolated revertants and mapped reversions. S. Y. performed genetic analyses of revertants. K. N. and K. O. directed the entire project and co-wrote the manuscript.

References

[1] Ueno, T., Oosawa, K. & Aizawa, S.-I. M Ring, S Ring and proximal rod of the flagellar basal body of *Salmonella typhimurium* are composed of subunits of a single protein, FliF. *J. Mol. Biol.* **227**, 672–677 (1992).

[2] Li, H. & Sourjik, V. Assembly and stability of flagellar motor in *Escherichia coli*. *Mol. Microbiol.* **80**, 886–899 (2011).

[3] Jones, C. J., Macnab, R. M., Okino, H. & Aizawa, S.-I. Stoichiometric analysis of the flagellar hook-(basal-body) complex of *Salmonella typhimurium*. *J. Mol. Biol.* **212**, 377–387 (1990).

[4] Sosinsky, G. E., Francis, N. R., DeRosier, D. J., Wall, J. S., Simon, M. N. & Hainfeld, J. Mass determination and estimation of subunit stoichiometry of the bacterial hook-basal body flagellar complex of *Salmonella typhimurium* by scanning transmission electron microscopy. *Proc. Natl. Acad. Sci. USA* **89**, 4801–4805 (1992).

[5] Suzuki, H., Yonekura, K. & Namba, K. Structure of the rotor of the bacterial flagellar motor revealed by electron cryomicroscopy and single-particle image analysis. *J. Mol. Biol.* **337**, 105–113 (2004).

[6] Thomas, D. R., Francis, N. R., Xu, C. & DeRosier, D. J. The three-dimensional structure of the flagellar rotor from a clockwise-locked mutant of *Salmonella enterica* serovar typhimurium. *J. Bacteriol.* **188**, 7039–7048 (2006).

[7] Braun, T. F., Al-Mawsawi, L. Q., Kojima, S. & Blair, D. F. Arrangement of core membrane segments in the MotA/MotB proton-channel complex of *Escherichia coli*. *Biochemistry* **43**, 35–45 (2004).

[8] Francis, N. R., Sosinsky, G. E., Thomas, D. & DeRosier, D. J. Isolation, characterization and structure of bacterial flagellar motors containing the switch complex. *J. Mol. Biol.* **235**, 1261–1270 (1994).

[9] Zhao, R. B., Amsler, C. D., Matsumura, P. & Khan, S. FliG and FliM distribution in the *Salmonella typhimurium* cell and flagellar basal bodies. *J. Bacteriol.* **178**, 258–265 (1996).

[10] Brown, P. N., Mathews, M. A. A, Joss, L. A., Hill, C. P. & Blair, D. F. Crystal structure of the flagellar rotor protein FIiN from *Thermotoga maritima*. *J. Bacteriol.* **187**, 2890–2902 (2005).

[11] Kihara, M., Miller, G. U. & Macnab, R. M. Deletion analysis of the flagellar switch protein FliG of *Salmonella*. *J. Bacteriol.* **182**, 3022–3028 (2000).

[12] Tang, H., Braun, T. F. & Blair, D. F. Motility protein complexes in the bacterial flagellar motor. *J. Mol. Biol.* **261**, 209–221 (1996).

[13] Lloyd, S. A., Tang, H., Wang, X., Billings, S. & Blair, D. F. Torque generation in the flagellar motor of *Escherichia coli*: Evidence of a direct role for FliG but not for FliM or FliN. *J. Bacteriol.* **178**, 223–231 (1996).

[14] Zhou, J. D., Lloyd, S. A. & Blair, D. F. Electrostatic interactions between rotor and stator in the bacterial flagellar motor. *Proc. Natl. Acad. Sci. USA* **95**, 6436–6441 (1998).

[15] Müller, V., Jones, C. J., Kawagishi, I., Aizawa, S.-I. & Macnab, R. M. Characterization of the *fliE* genes of *Escherichia coli* and *Salmonella typhimurium* and identification of the FliE protein as a component of the flagellar hook-basal body complex. *J. Bacteriol.* **174**, 2298–2304 (1992).

[16] Minamino, T., Yamaguchi, S. & Macnab, R. M. Interaction between FliE and FlgB, a proximal rod component of the flagellar basal body of *Salmonella*. *J. Bacteriol.* **182**, 3029–3036 (2000).

[17] Okino, H., Isomura, M., Yamaguchi, S., Magariyama, Y., Kudo, S. & Aizawa, S.-I. Release of flagellar Filament-Hook-Rod complex by a *Salmonella typhimurium* mutant defective in the M-ring of the basal body. *J. Bacteriol.* **171**, 2075–2082 (1989).

[18] Zhao, X., Zhang, K., Boquoi, T., Hu, B., Motaleb, M. A., Miller, K. A., *et al.* Cryoelectron tomography reveals the sequential assembly of bacterial flagella in *Borrelia burgdorferi*. *Proc. Natl. Acad. Sci. USA* **110**:14390–14395 (2013).

[19] Homma, M., DeRosier, D. J. & Macnab, R. M. Flagellar hook and hook-associated proteins of *Salmonella typhimurium* and their relationship to other axial components of the flagellum. *J. Mol. Biol.* **213**, 819–832 (1990).

[20] Mesibov, R. & Adler, J. Chemotaxis toward amino acids in *Escherichia coli*. *J. Bacteriol.* **112**, 315–326 (1972).

[21] Seymour, F. W. K. & Doetsch, R. N. Chemotactic responses by motile bacteria. *J. Gen. Microbiol.* **78**, 287–296 (1973).

[22] Tso, W. W. & Adler, J. Negative chemotaxis in *Escherichia coli*. *J. Bacteriol.* **118**, 560–576 (1974).

[23] Maeda, K., Imae, Y., Shioi, J.-I. & Oosawa, F. Effect of temperature on motility and chemotaxis of *Escherichia coli*. *J. Bacteriol.* **127**, 1039–1046 (1976).

[24] Imae, Y. Molecular mechanism of thermosensing in bacteria. in *Sensing and Response in Microorganisms*. (M. Eisenbach & M. Balaban eds.), pp. 73–81 (Amsterdam, Elsevier Science Publishes, 1985).

[25] Maddock, J. R. & Shapiro, L. Polar location of the chemoreceptor complex in the *Escherichia coli* cell. *Science* **259**, 1717–1723 (1993).

[26] Hess, J. F., Oosawa, K., Kaplan, N. & Simon, M. I. Phosphorylation of three proteins in the signaling pathway of bacterial chemotaxis. *Cell* **53**, 79–87 (1988).

[27] Oosawa, K., Hess, J. F. & Simon, M. I. Mutants defective in bacterial chemotaxis show modified protein phosphorylation. *Cell* **53**, 89–96 (1988).

[28] Turner, L., Ryu, W. S. & Berg, H. C. Real-time imaging of fluorescent flagellar filaments. *J. Bacteriol.* **182**, 2793–2801 (2000).

[29] Macnab, R. M. How bacteria assemble flagella. *Annu. Rev. Microbiol.* **57**, 77–100 (2003).

[30] Takeshita, S., Sato, M., Toba, M., Masahashi, W. & Hashimoto-Gotoh, T. High-copy-number and low-copy-number plasmid vectors for *lacZ* α-complementation and chloramphenicol- or kanamycin-resistance selection. *Gene* **61**, 63–74 (1987).

[31] Yamaguchi, S., Aizawa, S.-I., Kihara, M., Isomura, M., Jones, C. J. & Macnab, R. M. Genetic evidence for a switching and energy-transducing complex in the flagellar motor of *Salmonella typhimurium*. *J. Bacteriol.* **168**, 1172–1179 (1986).

[32] Yamaguchi, S., Fujita, H., Ishihara, A., Aizawa, S.-I. & Macnab, R. M. Subdivision of flagellar genes of *Salmonella typhimurium* into regions responsible for assembly, rotation, and switching. *J. Bacteriol.* **166**, 187–193 (1986).

[33] Kutsukake, K., Ohya, Y. & Iino, T. Transcriptional analysis of the flagellar regulon of *Salmonella typhimurium*. *J. Bacteriol.* **172**, 741–747 (1990).

[34] Kutsukake, K., Ikebe, T. & Yamamoto, S. Two novel regulatory genes, *fliT* and *fliZ*, in the flagellar regulon of *Salmonella*. *Genes Genet. Syst.* **74**, 287–292 (1999).

[35] Stafford, G. P. & Hughes, C. *Salmonella typhimurium flhE*, a conserved flagellar regulon gene required for swarming. *Microbiology* **153**, 541–547 (2007).

[36] Bochner, B. R., Huang, H. C., Schieven, G. L. & Ames, B. N. Positive selection for loss of tetracycline resistance. *J. Bacteriol.* **143**, 926–933 (1980).

[37] Jones, D. T. Protein secondary structure prediction based on position-specific scoring matrices. *J. Mol. Biol.* **292**, 195–202 (1999).

[38] Ueno, T., Oosawa, K. & Aizawa, S.-I. Domain structures of the MS ring component protein (FliF) of the flagellar basal body of *Salmonella typhimurium*. *J. Mol. Biol.* **236**, 546–555 (1994).

[39] Saijo-Hamano, Y., Uchida, N., Namba, K. & Oosawa, K. *In vitro* characterization of FlgB, FlgC, FlgF, FlgG, and FliE, flagellar basal body proteins of *Salmonella*. *J. Mol. Biol.* **339**, 423–435 (2004).

[40] Togashi, F., Yamaguchi, S., Kihara, M., Aizawa, S.-I. & Macnab, R. M. An extreme clockwise switch bias mutation in *fliG* of *Salmonella typhimurium* and its suppression by slow-motile mutations in *motA* and *motB*. *J. Bacteriol.* **179**, 2994–3003 (1997).

[41] Garza, A. G., Biran, R., Wohlschlegel, J. A. & Manson, M. D. Mutations in *motB* suppressible by changes in stator or rotor components of the bacterial flagellar motor. *J. Mol. Biol.* **258**, 270–285 (1996).

[42] Blair, D .F. & Berg, H. C. Mutations in the MotA protein of *Escherichia coli* reveal domains critical for proton conduction. *J. Mol. Biol.* **221**, 1433–1442 (1991).

[43] Zhou, J. D., Fazzio, R. T. & Blair, D. F. Membrane topology of the MotA protein of *Escherichia coli*. *J. Mol. Biol.* **251**, 237–242 (1995).

[44] Berg, H. C. The rotary motor of bacterial flagella. *Annu. Rev. Biochem.* **72**, 19–54 (2003).

[45] Kojima, S. & Blair, D. F. The bacterial flagellar motor: Structure and function of a complex molecular machine. *Int. Rev. Cytol.* **233**, 93–134 (2004).

[46] Sowa, Y. & Berry, R. M. Bacterial flagellar motor. *Q. Rev. Biophys.* **41**, 103–132 (2008).

[47] Blair, D. F. & Berg, H. C. The MotA protein of *Escherichia Coli* is a proton-conducting component of the flagellar motor. *Cell* **60**, 439–449 (1990).

[48] Stolz, B. & Berg, H. C. Evidence for interactions between MotA and MotB, torque-generating elements of the flagellar motor of *Escherichia coli*. *J. Bacteriol.* **173**, 7033–7037 (1991).

[49] Zhou, J. D., Sharp, L. L., Tang, H. L., Lloyd, S. A., Billings, S., Braun T. F., *et al.* Function of protonatable residues in the flagellar motor of *Escherichia coli*: a critical role for Asp 32 of MotB. *J. Bacteriol.* **180**, 2729–2735 (1998).

[50] Braun, T. F., Poulson, S., Gully, J. B., Empey, J. C., van Way, S., Putnam, A., *et al.* Function of proline residues of MotA in torque generation by the flagellar motor of *Escherichia coli*. *J. Bacteriol.* **181**, 3542–3551 (1999).

[51] Kojima, S. & Blair, D. F. Conformational change in the stator of the bacterial flagellar motor. *Biochemistry* **40**, 13041–13050 (2001).

[52] Che, Y. S., Nakamura, S., Kojima, S., Kami-Ike, N., Namba, K. & Minamino, T. Suppressor analysis of the MotB(D33E) mutation to probe bacterial flagellar motor dynamics coupled with proton translocation. *J. Bacteriol.* **190**, 6660–6667 (2008).

[53] Muramoto, K. & Macnab, R. M. Deletion analysis of MotA and MotB, components of the force-generating unit in the flagellar motor of *Salmonella*. *Mol. Microbiol.* **29**, 1191–1202 (1998).

[54] Morimoto, Y. V., Nakamura, S., Kami-ike, N., Namba, K. & Minamino, T. Charged residues in the cytoplasmic loop of MotA are required for stator assembly into the bacterial flagellar motor. *Mol. Microbiol.* **78**, 1117–1129 (2010).

[55] Morimoto, Y. V., Nakamura, S., Hiraoka, K. D., Namba, K. & Minamino, T. Distinct roles of highly conserved charged residues at the MotA-FliG interface in bacterial flagellar motor rotation. *J. Bacteriol.* **195**, 474–481 (2013).

[56] Hosking, E. R., Vogt, C., Bakker, E. P. & Manson, M. D. The *Escherichia coli* MotAB proton channel unplugged. *J. Mol. Biol.* **364**, 921–937 (2006).

[57] Kojima, S., Imada, K., Sakuma, M., Sudo, Y., Kojima, C., Minamino, T., *et al.* Stator assembly and activation mechanism of the flagellar motor by the periplasmic region of MotB. *Mol. Microbiol.* **73**, 710–718 (2009).

[58] Chun, S. Y. & Parkinson, J. S. Bacterial motility: membrane topology of the *Escherichia coli* MotB Protein. *Science* **239**, 276–278 (1988).

[59] De Mot, R. & Vanderleyden, J. The C-terminal sequence conservation between OmpA-related outer membrane proteins and MotB suggests a common function in both gram-positive

and gram-negative bacteria, possibly in the interaction of these domains with peptidoglycan. *Mol. Microbiol.* **12**, 333–334 (1994).

[60] Liu, X. Y. & Matsumura, P. The FlhD/FlhC complex, a transcriptional activator of the *Escherichia coli* flagellar class II operons. *J. Bacteriol.* **176**, 7345–7351 (1994).

[61] Claret, L. & Hughes, C. Functions of the subunits in the $FlhD_2C_2$ transcriptional master regulator of bacterial flagellum biogenesis and swarming. *J. Mol. Biol.* **303**, 467–478 (2000).

[62] Aldridge, P. & Hughes, K. T. Regulation of flagellar assembly. *Curr. Opin. Microbiol.* **5**, 160–165 (2002).

[63] Yamamoto, S. & Kutsukake, K. FliT acts as an anti-$FlhD_2C_2$ factor in the transcriptional control of flagellar regulon in *Salmonella enterica* serovar Typhimurium. *J. Bacteriol.* **188**, 6703–6708 (2006).

[64] Minamino, T., Imada, K., Kinoshita, M., Nakamura, S., Morimoto, Y. V. & Namba, K. Structural insight into the rotational switching mechanism of the bacterial flagellar motor. *PLoS Biol.* **9**, e1000616 (2011).

[65] Brown, P. N., Hill, C. P. & Blair, D. F. Crystal structure of the middle and C-terminal domains of the flagellar rotor protein FliG. *EMBO J.* **21**, 3225–3234 (2002).

[66] Brown, P. N., Terrazas, M., Paul, K. & Blair, D. F. Mutational analysis of the flagellar protein FliG: Sites of interaction with FliM and implications for organization of the switch complex. *J. Bacteriol.* **189**, 305–312 (2007).

[67] Paul, K., Gonzalez-Bonet, G., Bilwes, A. M., Crane, B. R. & Blair, D. Architecture of the flagellar rotor. *EMBO J.* **30**, 2962–2971 (2011).

[68] Lloyd, S. A. & Blair, D. F. Charged residues of the rotor protein FliG essential for torque generation in the flagellar motor of *Escherichia coli*. *J. Mol. Biol.* **266**, 733–744 (1997).

[69] Lee, L. K., Ginsburg, M. A., Crovace, C., Donohoe, M. & Stock, D. Structure of the torque ring of the flagellar motor and the molecular basis for rotational switching. *Nature* **466**, 996–1000 (2010).

[70] Marykwas, D. L. & Berg, H. C. A mutational analysis of the interaction between FliG and FliM, two components of the flagellar motor of *Escherichia coli*. *J. Bacteriol.* **178**, 1289–1294 (1996).

[71] Welch, M., Oosawa, K., Aizawa, S.-I. & Eisenbach, M. Phosphorylation-dependent binding of a signal molecule to the flagellar switch of bacteria. *Proc. Natl. Acad. Sci. USA* **90**, 8787–8791 (1993).

[72] Lee, S. Y., Cho, H. S., Pelton, J. G., Yan, D., Henderson, R. K., King, D. S., *et al.* Crystal structure of an activated response regulator bound to its target. *Nat. Struct. Biol.* **8**, 52–56 (2001).

[73] Dyer, C. M., Vartanian, A. S., Zhou, H. & Dahlquist, F. W. A molecular mechanism of bacterial flagellar motor switching. *J. Mol. Biol.* **388**, 71–84 (2009).

[74] Sarkar, M. K., Paul, K. & Blair, D. Chemotaxis signaling protein CheY binds to the rotor protein FliN to control the direction of flagellar rotation in *Escherichia coli*. *Proc. Natl. Acad. Sci. USA* **107**, 9370–9375 (2010).

[75] Park, S. Y., Lowder, B., Bilwes, A. M., Blair, D. F. & Crane, B. R. Structure of FliM provides insight into assembly of the switch complex in the bacterial flagella motor. *Proc. Natl. Acad. Sci. USA* **103**, 11886–11891 (2006).

[76] Paul, K., Brunstetter, D., Titen, S. & Blair, D. F. A molecular mechanism of direction switching in the flagellar motor of *Escherichia coli*. *Proc. Natl. Acad. Sci. USA* **108**, 17171–17176 (2011).

[77] Fukuoka, H., Inoue, Y., Terasawa, S., Takahashi, H. & Ishijima, A. Exchange of rotor components in functioning bacterial flagellar motor. *Biochem. Biophys. Res. Commun.* **394**, 130–135 (2010).

[78] Delalez, N. J., Wadhams, G. H., Rosser, G., Xue, Q., Brown, M. T., Dobbie, I. M., *et al.* Signal-dependent turnover of the bacterial flagellar switch protein FliM. *Proc. Natl. Acad. Sci. USA* **107**, 11347–11351 (2010).

[79] Sockett, H., Yamaguchi, S., Kihara, M., Irikura, V. M. & Macnab, R. M. Molecular analysis of the flagellar switch protein FliM of *Salmonella typhimurium*. *J. Bacteriol.* **174**, 793–806 (1992).

[80] Vogler, A. P., Homma, M., Irikura, V. M. & Macnab, R. M. *Salmonella typhimurium* mutants defective in flagellar filament regrowth and sequence similarity of FliI to F_0F_1, vacuolar, and archaebacterial ATPase subunits. *J. Bacteriol.* **173**, 3564–3572 (1991).

[81] Tang, H., Billings, S., Wang, X., Sharp, L. & Blair, D. F. Regulated underexpression and overexpression of the FliN Protein of *Escherichia Coli* and evidence for an interaction between FliN and FliM in the flagellar motor. *J. Bacteriol.* **177**, 3496–3503 (1995).